OPEN ACCESS

GAVIN PUBLISHERS

Food & Nutrition Journal

Research Article

Branton A, et al. Food Nutr J: FDNJ-188.
DOI: 10.29011/2575-7091. 100088

The Effect of Consciousness Energy Healing Treatment on the Physico-chemical and Thermal Properties of L-Cysteine

Alice Branton[1], Mahendra Kumar Trivedi[1], Dahryn Trivedi[1], Gopal Nayak[1], Snehasis Jana[2*]

[1]Trivedi Global, Inc., Henderson, USA

[2]Trivedi Science Research Laboratory Pvt. Ltd., Bhopal, India

[*]**Corresponding author:** Snehasis Jana, Trivedi Science Research Laboratory Pvt. Ltd., Bhopal, India. Tel: +912225811234; Email: publication@trivedieffect.com

Citation: Branton A, Trivedi MK, Trivedi D, Nayak G, Jana S (2018) The Effect of Consciousness Energy Healing Treatment on the Physicochemical and Thermal Properties of L-Cysteine. Food Nutr J: FDNJ-188. DOI: 10.29011/2575-7091. 100088

Received Date: 04 September, 2018; **Accepted Date:** 18 September, 2018; Published Date: 26 September, 2018

Abstract

L-cysteine is an essential amino acid and the basic building block of glutathione (denoted as the mother of all antioxidants). The aim of the study was to evaluate the impact of the Trivedi Effect®-Consciousness Energy Healing Treatment on the physicochemical and thermal properties of L-cysteine. The test sample was divided into control and treated samples. No treatment was given to the control sample, while the other portion remotely received the Biofield Treatment by a renowned Biofield Energy Healer, Alice Branton, and was termed as the treated sample. The particle size values were significantly reduced by 10.78%(d_{10}), 13.46%(d_{50}), 14.84%(d_{90}), and 13.95%{D(4, 3)}, thus, the specific surface area was significantly increased by 14.28% in the treated sample compared to the control sample. The PXRD peak intensities and crystallite sizes were significantly altered ranging from -79.18% to 335.64% and -82.68% to 294.32%, respectively; however, the average crystallite size was significantly reduced by 42.93% in the treated sample compared to the control sample. The latent heat of decomposition corresponding to 1st and 2nd peak of the treated sample was significantly reduced by 18.84% and 7.05%, respectively, compared with the control sample. The total weight loss was reduced by 2.53%; however, the residue weight was significantly increased by 784.73% in the treated sample in contrast to the control sample. Thus, the Biofield Treated L-cysteine might be more efficacious and advantageous to prepare pharmaceutical/nutraceutical dosage forms with improved solubility and bioavailability profile compared to the untreated sample, which can be used against various diseases/disorders such as bronchitis, COPD, psychosis, stress, aging, etc.

Keywords: Complementary and Alternative Medicine; Consciousness Energy Healing Treatment; L-cysteine; The Trivedi Effect®; PSA; PXRD; DSC; TGA

Introduction

L-cysteine is considered as an essential amino acid due to its less production by the human body. Thus, L-cysteine is consumed through the dietary supplements and is reported to have several health benefits. Vitamin B_6 and B_{12} are the major constituents needed for the production of L-cysteine the human body, which is generally manufactured from the amino acids viz. serine and methionine [1]. It was reported that L-cysteine is used by many ways; therapeutically and nutritionally, as it is the basic building block of glutathione (which is denoted as the mother of all antioxidants). N-acetyl-L-cysteine (NAC) is also used for the supplementation of L-cysteine, which has the ability to increase glutathione levels that is considered as one of the important factors for lung function, brain function, and liver detoxification. L-cysteine in the body is decreased due to various pathological health conditions; thus, it would be required externally to make more within your brain and body tissues. It helps to fight oxidative stress and its associated situations affecting brain and lungs [2]. It has several health benefits such as strong antioxidant properties [3], works as a free radical's scavenger, promotes body detoxification mechanism [4], increases male fertility by lowering oxidative stress [5], balances the blood sugar level [6], enhance body's digestive capacity by reducing aging process [7], relieves symptoms of respiratory health illness such as bronchitis or Chronic Obstructive Pulmonary Disease (COPD) [8], and also reported to treat psychiatric disorders [9]. Even though, it can be obtained from the different foods such as cheese, yogurt, pork, chicken, turkey, duck, wheat germ, and oats, the rate of absorption and mechanism of action of any compound depends upon numerous factors such as its solubility, stability, pharmacokinetics, and bioavailability. The physicochemical

properties of any amino acids are very important to show their biological property and actions. Therefore, this research has been carried out to improve the physicochemical properties (particle size, crystalline structure, crystallite size, surface area, etc.) of L-cysteine.

The Biofield Energy Treatment is one of the best Complementary and Alternative Medicine (CAM) approaches that significantly defines a unique concept between the traditional and contemporary explanatory models of energy medicine [10]. The Biofield Energy Healing Treatment has provided significant outcomes in both clinical practice and scientific research focusing in the field of energy medicine of the body [11,12]. Biofield Energy Healing has been considered as an Energy therapy and is accepted by the National Institutes of Health (NIH) and National Center for Complementary and Alternative Medicine (NCCAM) along with other therapies, which include traditional Chinese herbs and medicines, Ayurvedic medicine, naturopathy, homeopathy, yoga, acupuncture, acupressure, meditation, Tai Chi, Qi Gong, chiropractic/osteopathic manipulation, healing touch, Reiki, deep breathing, special diets, massage, progressive relaxation, relaxation techniques, guided imagery, movement therapy, hypnotherapy, pilates, Rolfing structural integration, mindfulness, cranial sacral therapy, aromatherapy, and applied prayer [13]. The Trivedi Effect®-Consciousness Energy Healing Treatment has been described worldwide to have remarkable results in non-living materials and in living organisms. Biofield Energy Healing Treatments have significantly altered the physicochemical and thermal properties of many pharmaceutical/nutraceutical compounds [14-16], altered characteristics properties of micro-organisms [17-19], crops [20,21], livestock [22], metals, ceramics [23,24], plant growth and adaptation [25], human health and wellness [26-29].

Thus, this study was also aimed to analyse the impact of the Biofield Energy Healing Treatment (The Trivedi Effect®) on the physicochemical and thermal properties of ascorbic acid by using various analytical techniques such as, Particle Size Analysis (PSA), Powder X-Ray Diffraction (PXRD), Thermogravimetric Analysis (TGA)/ Differential Thermogravimetric Analysis (DTG), and Differential Scanning Calorimetry (DSC).

Materials and Methods

Chemicals and Reagents

L-cysteine was purchased from Alfa Aesar, USA. All other chemicals used during the experiments were of analytical grade available in India.

Consciousness Energy Healing Treatment Strategies

L-cysteine, *i.e.,* the test compound was divided into two parts. Among both parts, one portion was denoted as control sample that did not receive the Biofield Energy Treatment. The other part of L-cysteine was considered as the treated part that received the Energy of Consciousness Healing Treatment by the renowned Biofield Energy Healer, Alice Branton (USA), and was named as the Biofield Energy Treated sample. In the process of the Biofield Energy Treatment, the sample was kept under the standard laboratory conditions, and the Biofield Energy Healer provided the Trivedi Effect®-Energy of Consciousness Healing Treatment to the sample, remotely, for 3 minutes through the Unique Energy Transmission process. The control L-cysteine was subjected to "sham" healer under the similar laboratory conditions, who did not have any knowledge about the Biofield Energy Healing Treatment. After the treatment, both the samples were kept in similar sealed conditions and further characterized by using PSA, PXRD, DSC, and TGA/DTG techniques.

Characterization

Particle Size Analysis (PSA)

The particle size analysis of L-cysteine was conducted on Malvern Mastersizer 2000, from the UK, with a detection range between 0.01 µm to 3000 µm using wet method [30,31]. The sample unit (Hydro MV) was filled with a dispersant medium (sunflower oil) and operated the stirrer at 2500 rpm. The PSA analysis of L-cysteine was performed to obtain the average particle size distribution. Where, d (0.1) µm, d(0.5) µm, d(0.9) µm represent particle diameter corresponding to 10%, 50%, and 90% of the cumulative distribution. D(4,3) represents the average mass-volume diameter, and SSA is the specific surface area (m^2/g). The calculations were done by using software Mastersizer Ver. 5.54.

The percent change in particle size (d) for L-cysteine at below 10% level (d_{10}), 50% level (d_{50}), 90% level (d_{90}), and D(4,3) was calculated using the following equation 1:

$$\% \text{ change in particle size} = \frac{[d_{Treated} - d_{Control}]}{d_{Control}} \times 100 \quad (1)$$

Where $d_{Control}$ and $d_{Treated}$ are the particle sizes (µm) at below 10% level (d_{10}), 50% level (d_{50}), and 90% level (d_{90}) of the control and the Biofield Energy Treated samples, respectively.

The percent change in surface area (S) was calculated using the following equation 2:

$$\% \text{ change in surface area} = \frac{[S_{Treated} - S_{Control}]}{S_{Control}} \times 100 \quad (2)$$

Where $S_{Control}$ and $S_{Treated}$ are the surface area of the control and the Biofield Energy Treated L-cysteine, respectively.

Powder X-ray Diffraction (PXRD) Analysis

The PXRD analysis of L-cysteine was performed with the help of RigakuMiniFlex-II Desktop X-ray diffractometer (Japan) [32,33]. The Cu Kα radiation source tube output voltage used was 30 kV and tube output current were 15 mA. Scans were performed

at room temperature. The average size of individual crystallites was calculated from XRD data using the Scherrer's formula (3)

$$G = k\lambda/\beta\cos\theta \quad (3)$$

Where k is the equipment constant (0.94), G is the crystallite size in nm, λ is the radiation wavelength (0.154056 nm for Kα1 emission), β is the full-width at half maximum (FWHM), and θ is the Bragg angle [34].

The percent change in crystallite size (G) of L-cysteine was calculated using the following equation 4:

$$\%\ \text{change in crystallite size} = \frac{[G_{Treated} - G_{Control}]}{G_{Control}} \times 100 \quad (4)$$

Where $G_{Control}$ and $G_{Treated}$ are the crystallite size of the control and the Biofield Energy Treated samples, respectively.

Differential Scanning Calorimetry (DSC)

The DSC analysis of L-cysteine was performed with the help of DSC Q200, TA instruments. Sample of ~1-5 mg was loaded to the aluminium sample pan at a heating rate of 10˚C/min from 30˚C to 350˚C [30,31]. The % change in melting point (T) was calculated using the following equation 5:

$$\%\ \text{change in melting point} = \frac{[T_{Treated} - T_{Control}]}{T_{Control}} \times 100 \quad (5)$$

Where $T_{Control}$ and $T_{Treated}$ are the melting point of the control and treated samples, respectively.

The percent change in the latent heat of decomposition (ΔH) was calculated using following equation 6:

$$\%\ \text{change in latent heat of decomposition} = \frac{[\Delta H_{Treated} - \Delta H_{Control}]}{\Delta H_{Control}} \times 100 \quad (6)$$

Where $\Delta H_{Control}$ and $\Delta H_{Treated}$ are the latent heat of decomposition of the control and treated L-cysteine, respectively.

Thermal Gravimetric Analysis (TGA)/ Differential Thermogravimetric Analysis (DTG)

TGA/DTG thermograms of L-cysteine were obtained with the help of TGA Q50 TA instruments. A sample of 5 mg was loaded to the platinum crucible at a heating rate of 10˚C/min from 25˚C to 1000˚C with the recent literature [30,31]. The % change in weight loss (W) was calculated using the following equation 7:

$$\%\ \text{change in weight loss} = \frac{[W_{Treated} - W_{Control}]}{W_{Control}} \times 100 \quad (7)$$

Where $W_{Control}$ and $W_{Treated}$ are the weight loss of the control and the Biofield Energy Treated L-cysteine, respectively.

The % change in maximum thermal degradation temperature (T_{max}) (M) was calculated using the following equation 8:

$$\%\ \text{change in Tmax (M)} = \frac{[M_{Treated} - M_{Control}]}{M_{Control}} \times 100 \quad (8)$$

Where $M_{Control}$ and $M_{Treated}$ are the T_{max} values of the control and the Biofield Energy Treated L-cysteine, respectively.

Results and Discussion

Particle Size Analysis (PSA)

The analysis of particle size of the control and the Biofield Energy Treated L-cysteine samples are presented in Table 1, which showed that the particle size distribution of the control sample at d_{10}, d_{50}, d_{90}, and D(4, 3) were 263.81 µm, 497.33 µm, 910.97 µm, and 547.66 µm, respectively. Besides, the particle size at d_{10}, d_{50}, d_{90}, and D(4, 3) of the Biofield Energy Treated sample was found as 235.36 µm, 430.37 µm, 775.77 µm, and 471.25 µm, respectively. The overall analysis revealed the reduction in the particle size values of the Biofield Energy Treated L-cysteine sample by 10.78%, 13.46%, 14.84%, and 13.95% at d_{10}, d_{50}, d_{90}, and D(4, 3), respectively, compared to the control sample.

Parameter	d_{10} (µm)	d_{50} (µm)	d_{90} (µm)	D(4,3)(µm)	SSA(m^2/g)
Control	263.81	497.33	910.97	547.66	0.014
Biofield Treated	235.36	430.37	775.77	471.25	0.016
Percent change* (%)	-10.78	-13.46	-14.84	-13.95	14.28

d_{10}, d_{50}, and d_{90}: particle diameter corresponding to 10%, 50%, and 90% of the cumulative distribution, D(4,3): the average mass-volume diameter, and SSA: the specific surface area. *denotes the percentage change in the Particle size distribution of the Biofield Energy Treated sample with respect to the control sample.

Table 1: Particle size distribution of the control and the Biofield Energy Treated L-cysteine.

Moreover, the specific surface area of the Biofield Energy Treated sample was observed as 0.016 m^2/g, which was increased by 14.28% as compared with the SSA of the control sample (0.014 m^2/g). The particle size and surface area of drug moiety are considered important factors regarding its solubility, dissolution, and bioavailability as well as its performance within the body [35,36]. Studies reported the improvement in the absorption and bioavailability profile of drug as a result of the reduction in particle

size and increase in its surface area [37]. Thus, the Biofield Energy Treated L-cysteine might possess improved solubility, dissolution rate, and bioavailability as compared to the untreated sample.

Powder X-ray Diffraction (PXRD) Analysis

The control and the Biofield Energy Treated L-cysteine samples showed the presence of sharp and intense peaks in the diffractograms (Figure 1). Such peaks indicated the crystalline nature of the control and the Biofield Energy Treated samples; however, there were some alterations in the Bragg's angle of the characteristic peaks of the treated sample as compared to the control L-cysteine sample. Moreover, the analysis of the intensities and the crystallite size was done for both the control and the Biofield Energy Treated sample (Table 2). The diffractogram revealed the highest peak intensity (100%) in the control sample at 2θ equal to 24.71°, while it was observed at 24.86° in the Biofield Energy Treated sample. Also, the diffractogram of the Biofield Energy Treated sample showed a new peak at 42.30°; whereas, the peak at 2θ equal to 34.12° in the control sample was not observed in it. Besides, the Biofield Energy Treated L-cysteine sample showed alteration in the intensities of the diffraction peaks ranging from -79.18% to 335.64% as compared to the control sample. These significant changes in the intensities of the characteristic diffraction peaks indicated the alterations in the crystallinity of the Biofield Energy Treated sample in comparison to the control sample.

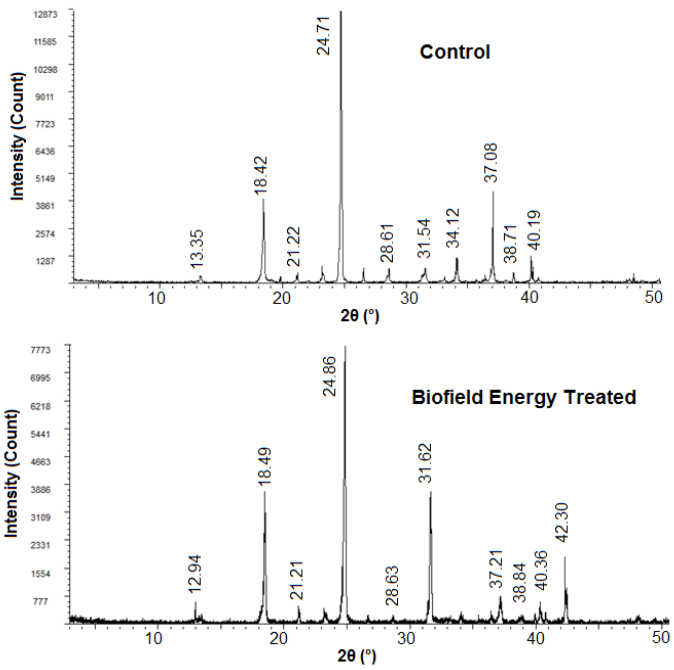

Figure 1: PXRD diffractograms of the control and the Biofield Energy Treated L-cysteine.

Entry No.	Bragg angle (°2θ)		Intensity (cps)			Crystallite size (G, nm)		
	Control	Treated	Control	Treated	% change [a]	Control	Treated	% change [b]
1	13.35	12.94	54	15	-72.22	511	2015	294.32
2	18.42	18.49	500	448	-10.40	966	660	-31.68
3	21.22	21.21	14	34.4	145.71	4849	840	-82.68
4	24.71	24.86	1316	943	-28.34	980	504	-48.57
5	28.61	28.63	73	15.2	-79.18	817	466	-42.96
6	31.54	31.62	101	440	335.64	704	766	8.81
7	37.08	37.21	212	104	-50.94	2101	420	-80.01
8	38.71	38.84	28	11.6	-58.57	1207	1255	3.98
9	40.19	40.36	74	51	-31.08	1384	789	-42.99

[a]denotes the percentage change in the intensity of the Biofield Energy Treated sample with respect to the control sample; [b]denotes the percentage change in the crystallite size of Biofield Energy Treated sample with respect to the control sample.

Table 2: PXRD data for the control and the Biofield Energy Treated L-cysteine.

Moreover, the significant alterations were also observed in the crystallite sizes of the Biofield Energy Treated sample ranging from -82.68% to 294.32% as compared to the control sample. Apart from that, there was 42.93% reduction in the average crystallite size of the Biofield Energy Treated L-cysteine sample (857.22 nm) as compared to the control sample (1502.11 nm). The previous studies showed the significant impact of the Biofield Energy Treatment on the crystal morphology as well as the crystalline

structure of various compounds in terms of the alterations in their peak intensities and crystallite sizes, etc. Such changes might also take place due to the formation of a new polymorphic form of the compound after the Biofield Energy Treatment [38,39]. Hence, it could be assumed that the significant alterations in the crystallite size along with the peak intensities of the characteristic peaks of the Biofield Energy Treated sample might have happened due to the formation of a new polymorph of L-cysteine *via* the mediation of neutrino oscillations [40-41]. Various studies reported that the physical modifications such as altering the crystal habit of the drug might help in improving the bioavailability profile of drug [40]. Thus, it is presumed that the Biofield Energy Treated sample might possess better solubility, dissolution and bioavailability profile than the untreated sample.

Differential Scanning Calorimetry (DSC) Analysis

The DSC thermograms shown in figure 2 revealed the melting and other thermal behaviours of the control and the Biofield Energy Treated L-cysteine samples [42]. According to the literature, the amino acids undergo the process of thermal decomposition instead of sublimation or melting. Also, the peak in DSC thermogram was accompanied by the drop in the TGA thermogram at the same temperature. The coinciding of DSC peak with the TGA drop indicated the simple decomposition process that took place during the heating of L-cysteine sample [42,43]. The thermograms of both, the control and the Biofield Energy Treated sample showed two peaks. The decomposition temperature of the 1st and 2nd peak of the Biofield Energy Treated L-cysteine sample were slightly altered by 0.57% and -0.22%, respectively as that of the control sample. However, the latent heat of decomposition ($\Delta H_{decomposition}$) corresponding to 1st and 2nd peak of the Biofield Energy Treated sample was significantly reduced by 18.84% and 7.05%, respectively, as compared to the control sample (Table 3).

Peak	Description	Melting Point (˚C)	$\Delta H_{decomposition}$ (J/g)
Peak 1	Control sample	177.40	24.73
	Biofield Treated sample	178.42	20.07
	% Change*	0.57	-18.84
Peak 2	Control sample	222.15	608.70
	Biofield Treated sample	221.65	565.80
	% Change*	-0.22	-7.05

ΔH: Latent heat of decomposition; *denotes the percentage change of the Biofield Energy Treated sample with respect to the control sample.

Table 3: Comparison of DSC data between the control and the Biofield Energy Treated L-cysteine.

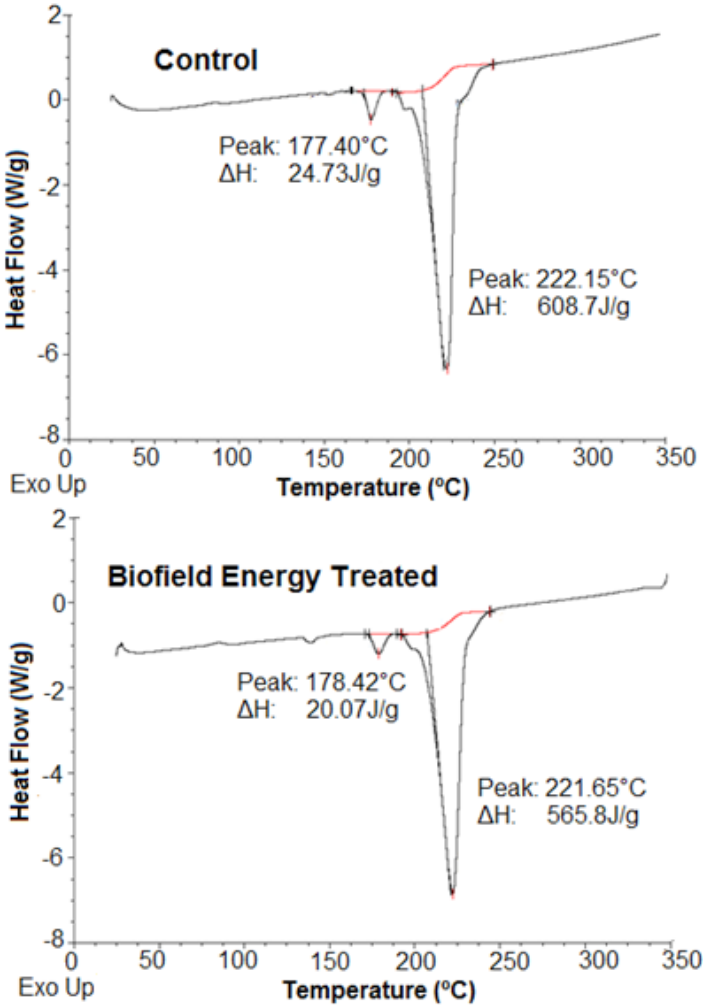

Figure 2: DSC thermograms of the control and the Biofield Energy Treated L-cysteine.

The analysis revealed that the degradation temperature for both, the control and the Biofield Energy Treated samples remained same; however, there might be some alterations in the crystallization structure of the L-cysteine [42] after the Biofield Energy Treatment that might cause the alteration in the $\Delta H_{decomposition}$ of the treated sample as compared to the untreated one.

Thermal Gravimetric Analysis (TGA)/ Differential thermogravimetric analysis (DTG)

The TGA thermograms (Figure 3) of the control and the Biofield Energy Treated samples showed thermal degradation of L-cysteine in a single step. Also, the degradation temperature was found similar to the reported literature [44]. The analysis of thermograms revealed that the total weight loss of the Biofield Energy Treated sample was 97.16%, which was reduced by 2.53% as compared with the control sample (99.68%). It resulted in the significant increase in residue amount of the treated L-cysteine sample by 784.73% when compared to the control sample (Table 4). Thus, it showed that the thermal stability of the treated L-cysteine was improved as compared to the untreated sample.

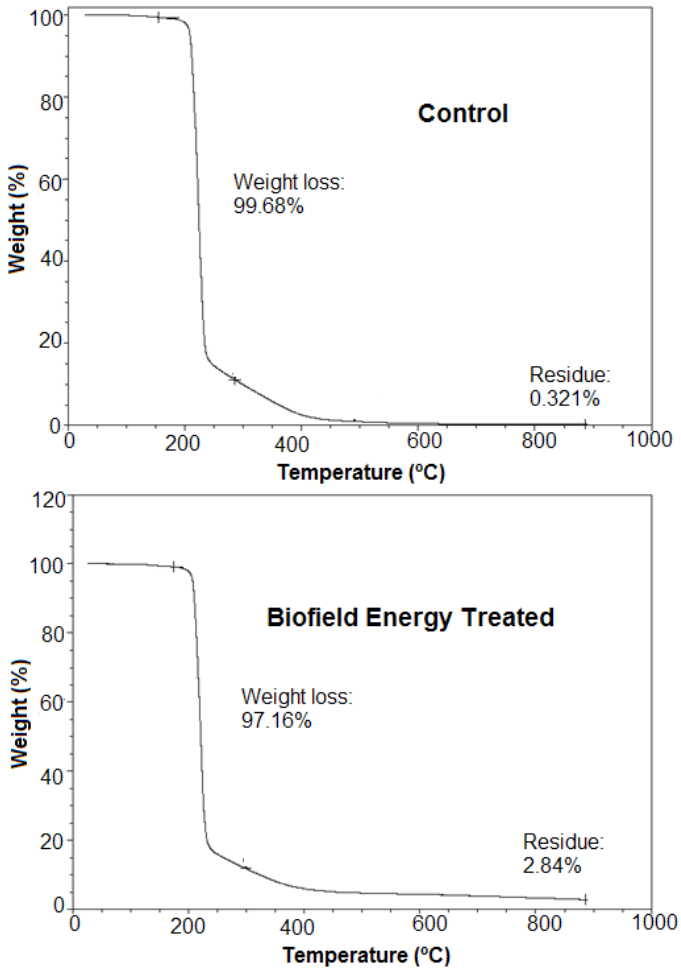

Figure 3: TGA thermograms of the control and the Biofield Energy Treated L-cysteine.

Sample	TGA		DTG
	Total weight loss (%)	Residue %	T_{max} (°C)
Control	99.68	0.321	224.26
Biofield Energy Treated	97.16	2.840	220.73
% Change*	-2.53	784.73	-1.57

*denotes the percentage change of the Biofield Energy Treated sample with respect to the control sample, T_{max} = the temperature at which maximum weight loss takes place in TG or peak temperature in DTG.

Table 4: TGA/DTG data of the control and the Biofield Energy Treated samples of L-cysteine.

Moreover, the DTG analysis of the control and the Biofield Energy Treated L-cysteine sample revealed the presence of a single peak in the thermogram (Figure 4). The further analysis showed that the maximum thermal degradation temperature (T_{max}) of the Biofield Energy Treated sample was reduced by 1.57% in comparison to the control sample (Table 4). Hence, the TGA/DTG study revealed the altered thermal stability of the Biofield Energy Treated L-cysteine sample as compared with the control sample.

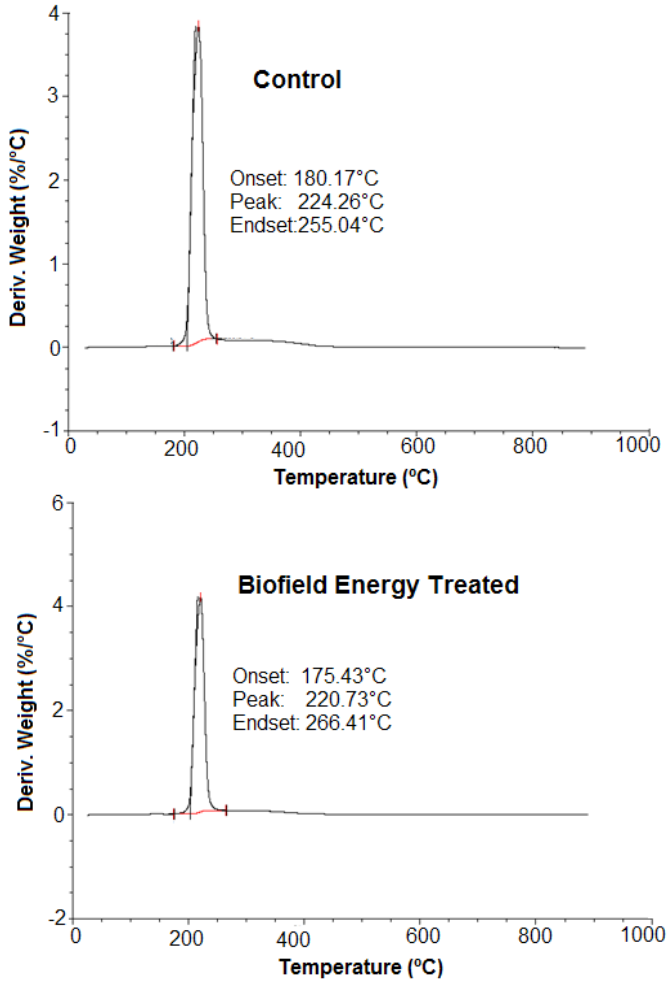

Figure 4: DTG thermograms of the control and the Biofield Energy Treated L-cysteine.

Conclusion

The study results showed that the Trivedi Effect®-Consciousness Energy Healing Treatment significantly impacted the physicochemical and thermal properties of L-cysteine such as particle size distribution, crystallite sizes, latent heat, etc. The particle size values of the Biofield Energy Treated L-cysteine at d_{10}, d_{50}, d_{90}, and D(4, 3) were observed to be significantly reduced by 10.78%, 13.46%, 14.84%, and 13.95%, respectively, compared to the control sample. It resulted in the increase of the specific surface area of the Biofield Energy Treated L-cysteine by 14.28% as compared to the untreated sample. The reduction in particle sizes and increase in the surface area might help in improving the solubility and dissolution rate of L-cysteine that further enhances its absorption and bioavailability profile in the body. The PXRD peak intensities and crystallite sizes of those peaks of the Biofield Energy Treated L-cysteine sample showed significant alterations ranging from -79.18% to 335.64% and -82.68% to 294.32%, respectively as compared to the untreated sample. Also, the Biofield Energy Treatment affected the average crystallite size of the Biofield Energy Treated L-cysteine sample that was observed to be significantly reduced by 42.93%, compared to the control sample. The Biofield Energy Treated sample showed slight alterations in the peak temperatures corresponding to 1st and 2nd peak by 0.57% and -0.22%, respectively in comparison to the untreated sample. However, the $\Delta H_{decomposition}$ corresponding to 1st and 2nd peak was significantly reduced by 18.84% and 7.05%, respectively, as compared to the untreated L-cysteine sample. The total weight loss was reduced by 2.53%, however, the residue amount was significantly increased by 784.73% in the Biofield Energy Treated L-cysteine compared with the control sample. Besides, the T_{max} of the treated L-cysteine sample was decreased by 1.57%, compared with the control sample. Hence, the thermal analysis data indicated that there was a significant alteration in the thermal stability of the Biofield Energy Treated sample in comparison to the control sample. Overall, the Trivedi Effect®-Consciousness Energy Healing Treatment was found to have a significant impact on the L-cysteine sample that might help in improving the absorption and bioavailability profile of it by generating its new polymorphic form, altering its crystallinity, reducing the particle size, and improving the surface area. Such alterations in the Trivedi Effect® Treated L-cysteine can show the better performance in its different formulation forms, which might offer better therapeutic response against various diseases and disorders, i.e., respiratory health illness, bronchitis, COPD, psychiatric disorders, reducing aging process, balancing blood sugar, etc.

Acknowledgements

The authors are grateful to Central Leather Research Institute, SIPRA Lab. Ltd., Trivedi Science, Trivedi Global, Inc., Trivedi Testimonials, and Trivedi Master Wellness for their assistance and support during this work.

Conflict of Interest

Authors declare no conflict of interest.

References

1. Mokhtari V, Afsharian P, Shahhoseini M, Kalantar SM, Moini A (2017) A review on various uses of N-acetyl cysteine. Cell J 19: 11-17.
2. Kelly GS (1998) Clinical applications of N-acetylcysteine. Altern Med Rev 3: 114-127.
3. Shackebaei D, King N, Shukla B, Suleiman MS (2005) Mechanisms underlying the cardioprotective effect of L-cysteine. Mol Cell Biochem 277: 27-31.
4. Quig D (1998) Cysteine metabolism and metal toxicity. Altern Med Rev 3: 262-270.
5. Barekat F, Tavalaee M, Deemeh MR, Bahreinian M, Azadi L, et al. (2016) A Preliminary study: N-acetyl-L-cysteine improves semen quality following varicocelectomy. Int J Fertil Steril 10: 120-126.
6. Jain SK, Velusamy T, Croad JL, Rains JL, Bull R (2009) L-cysteine supplementation lowers blood glucose, glycated hemoglobin, CRP, MCP-1, oxidative stress and inhibits NFkB activation in the livers of Zucker diabetic rats. Free Radic Biol Med 46: 1633-1638.
7. Guijarro LG, Mate J, Gisbert JP, Perez-Calle JL, Marin-Jimenez I, et al. (2008) N-acetyl-L-cysteine combined with mesalamine in the treatment of ulcerative colitis: Randomized, placebo-controlled pilot study. World J Gastroenterol 14: 2851-2857.
8. Dekhuijzen P, van Beurden W (2006) The role for N-acetylcysteine in the management of COPD. Int J Chron Obstruct Pulmon Dis 1: 99-106.
9. Dean O, Giorlando F, Berk M (2011) N-acetylcysteine in psychiatry: Current therapeutic evidence and potential mechanisms of action. J Psychiatry Neurosci 36: 78-86.
10. Guarneri E, King RP (2015) Challenges and opportunities faced by biofield practitioners in global health and medicine: A white paper. Global Advances in Health and Medicine 4: 89-96.
11. Barnes PM, Bloom B, Nahin RL (2008) Complementary and alternative medicine use among adults and children: United States, 2007. Natl Health Stat Report 12: 1-23.
12. Frass M, Strassl RP, Friehs H, Müllner M, Kundi M, et al. (2012) Use and acceptance of complementary and alternative medicine among the general population and medical personnel: A systematic review. Ochsner J 12: 45-56.
13. Koithan M (2009) Introducing complementary and alternative therapies. J Nurse Pract 5: 18-20.
14. Trivedi MK, Branton A, Trivedi D, Shettigar H, Bairwa K, et al. (2015) Fourier transform infrared and ultraviolet-visible spectroscopic characterization of biofield treated salicylic acid and sparfloxacin. Nat Prod Chem Res 3: 186.
15. Trivedi MK, Branton A, Trivedi D, Nayak G, Nykvist CD, et al. (2017) Evaluation of the Trivedi Effect®- Energy of Consciousness Energy Healing Treatment on the physical, spectral, and thermal properties of zinc chloride. American Journal of Life Sciences. 5: 11-20.
16. Trivedi MK, Patil S, Shettigar H, Bairwa K, Jana S (2015) Spectroscopic characterization of biofield treated metronidazole and tinidazole. Med chem 5: 340-344.
17. Trivedi MK, Patil S, Shettigar H, Mondal SC, Jana S (2015) Evaluation of biofield modality on viral load of Hepatitis B and C viruses. J Antivir Antiretrovir 7: 083-088.
18. Trivedi MK, Branton A, Trivedi D, Nayak G, Charan S, et al. (2015) Phenotyping and 16S rDNA analysis after biofield treatment on *Citrobacter braakii*: A urinary pathogen. J Clin Med Genom 3: 129.
19. Trivedi MK, Patil S, Shettigar H, Mondal SC, Jana S (2015) An impact of biofield treatment: Antimycobacterial susceptibility potential using BACTEC 460/MGIT-TB System. Mycobact Dis 5: 189.
20. Trivedi MK, Branton A, Trivedi D, Nayak G, Mondal SC, et al. (2015) Morphological characterization, quality, yield and DNA fingerprinting of biofield energy treated alphonso mango (*Mangifera indica* L.). Journal of Food and Nutrition Sciences 3: 245-250.
21. Trivedi MK, Branton A, Trivedi D, Nayak G, Mondal SC, et al. (2015) Evaluation of biochemical marker - glutathione and DNA fingerprinting of biofield energy treated *Oryza sativa*. American Journal of BioScience 3: 243-248.
22. Trivedi MK, Branton A, Trivedi D, Nayak G, Mondal SC, et al. (2015) Effect of biofield treated energized water on the growth and health status in chicken (*Gallus gallus domesticus*). Poult Fish WildlSci 3: 140.
23. Trivedi MK, Tallapragada RM, Branton A, Trivedi D, Nayak G, et al. (2015) Analysis of physical, thermal, and structural properties of biofield energy treated molybdenum dioxide. International Journal of Materials Science and Applications 4: 354-359.
24. Trivedi MK, Tallapragada RM, Branton A, Trivedi D, Nayak G, et al. (2015) The potential impact of biofield energy treatment on the physical and thermal properties of silver oxide powder. International Journal of Biomedical Science and Engineering 3: 62-68.
25. Nayak G, Altekar N (2015) Effect of biofield treatment on plant growth and adaptation. J Environ Health Sci 1: 1-9.
26. Branton A, Jana S (2017) The influence of energy of consciousness healing treatment on low bioavailable resveratrol in male Sprague Dawley rats. International Journal of Clinical and Developmental Anatomy 3: 9-15.
27. Kinney JP, Trivedi MK, Branton A, Trivedi D, Nayak G, et al. (2017) Overall skin health potential of the biofield energy healing based herbomineral formulation using various skin parameters. American Journal of Life Sciences 5: 65-74.
28. Branton A, Jana S (2017) Effect of The biofield energy healing treatment on the pharmacokinetics of 25-hydroxyvitamin D_3 [25(OH)D_3] in rats after a single oral dose of vitamin D_3. American Journal of Pharmacology and Phytotherapy 2: 11-18.
29. Singh J, Trivedi MK, Branton A, Trivedi D, Nayak G, et al. (2017) Consciousness energy healing treatment based herbomineral formulation: A safe and effective approach for skin health. American Journal of Pharmacology and Phytotherapy 2: 1-10.
30. Trivedi MK, Sethi KK, Panda P, Jana S (2017) Physicochemical, thermal and spectroscopic characterization of sodium selenate using XRD, PSD, DSC, TGA/DTG, UV-vis, and FT-IR. Marmara Pharmaceutical Journal 21/2: 311-318.
31. Trivedi MK, Sethi KK, Panda P, Jana S (2017) A comprehensive physicochemical, thermal, and spectroscopic characterization of zinc (II) chloride using X-ray diffraction, particle size distribution, differential scanning calorimetry, thermogravimetric analysis/differential thermo-

gravimetric analysis, ultraviolet-visible, and Fourier transform-infrared spectroscopy. International Journal of Pharmaceutical Investigation 7: 33-40.

32. Zhang T, Paluch K, Scalabrino G, Frankish N, Healy AM, et al. (2015) Molecular structure studies of (1S,2S)-2-benzyl-2,3-dihydro-2-(1Hinden-2-yl)-1H-inden-1-ol. J Mol Struct 1083: 286-299.

33. Desktop X-ray Diffractometer “MiniFlex+” (1997) The Rigaku Journal 14: 29-36.

34. Langford JI, Wilson AJC (1978) Scherrer after sixty years: A survey and some new results in the determination of crystallite size. J Appl Cryst 11: 102-113.

35. Loh ZH, Samanta AK, Heng PWS (2015) Overview of milling techniques for improving the solubility of poorly water-soluble drugs. Asian J Pharm 10: 255-274.

36. Khadkaa P, Roa J, Kim H, Kim I, Kim JT, et al. (2014) Pharmaceutical particle technologies: An approach to improve drug solubility, dissolution and bioavailability. Asian J Pharm 9: 304-316.

37. Hu J, Johnston KP, Williams RO (2004) Nanoparticle engineering processes for enhancing the dissolution rates of poorly water-soluble drugs. Drug Dev Ind Pharm 30: 233-245.

38. Trivedi MK, Branton A, Trivedi D, Nayak G, Lee AC, et al. (2017) Evaluation of the impact of biofield energy healing treatment (The Trivedi Effect®) on the physicochemical, thermal, structural, and behavioural properties of magnesium gluconate. International Journal of Nutrition and Food Science 6: 71-82.

39. Trivedi MK, Branton A, Trivedi D, Nayak G, Plikerd WD, et al. (2017) Evaluation of the physicochemical, spectral, thermal and behavioral properties of sodium selenate: Influence of the energy of consciousness healing treatment. American Journal of Quantum Chemistry and Molecular Spectroscopy 2: 18-27.

40. Savjani KT, Gajjar AK, Savjani JK (2012) Drug solubility: Importance and enhancement techniques. ISRN Pharmaceutics, 2012: Article ID 195727.

41. Trivedi MK, Mohan TRR (2016) Biofield energy signals, energy transmission and neutrinos. American Journal of Modern Physics 5: 172-176.

42. Zhao Z, Xie M, Li Y, Chen A, Li G, et al. (2015) Formation of curcumin nanoparticles via solution enhanced dispersion by supercritical CO_2. Int J Nanomedicine 10: 3171-3181.

43. Weiss IM, Muth C, Drumm R, Kirchner HOK (2018) Thermal decomposition of the amino acids glycine, cysteine, aspartic acid, asparagine, glutamic acid, glutamine, arginine and histidine. BMC Biophysics 11: 2.

44. Mohammed AV, Arulappan JAP, Ganesan ST, Sagadevan S (2015) Analysis on the growth and characterization of a non-linear optical single crystal: L-cystine dihydrobromide. Mat Res 18: 828-832.